Turbulence

Michael Shats and Hua Xia
The Australian National University, Canberra, Australia

1 INTRODUCTION

There is no universal definition of turbulence agreed to by the entire scientific community. The reasons for this are multiple. Firstly, there is no comprehensive theory of turbulence. It is recognized as one of the outstanding problems in physics despite focused efforts for over 100 years. Secondly, because turbulence is important in many disciplines, different aspects of turbulence are of interest for different specialists. As such, the question "what is really important" with regard to turbulence is answered differently by engineers, oceanographers, atmospheric scientists, plasma physicists, astrophysicists, and so on.

Encyclopedia of Maritime and Offshore Engineering, online © 2017 John Wiley & Sons, Ltd.

DOI: 10.1002/9781118476406.emoe074
Also published in the *Encyclopedia of Maritime and Offshore Engineering* (print edition)
ISBN: 978-1-118-47635-2

A good starting point is this relatively neutral definition given in the Encyclopedia of Nonlinear Science (Scott, 2005):

> Turbulence is a state of a nonlinear physical system that has energy distribution over many degrees of freedom strongly deviated from equilibrium. Turbulence is irregular both in time and in space. Turbulence can be maintained by some external influence or it can decay on the way to relaxation to equilibrium. The term first appeared in fluid mechanics and was later generalized to include far-from-equilibrium states in solids and plasmas.

A classical example, which illustrates the onset of turbulence, was described in 1883 by Reynolds (1883) who studied a flow in a narrow circular pipe. By visualizing the water flow using thin lines of a dye, Reynolds found that at low velocities the dye streaks represented straight lines, while at higher velocities the onset of distinct curls marked a transition to a turbulent motion. This transition occurs at sufficiently large values of the Reynolds number $Re \equiv V d/\nu > 2 \times 10^3$. Here, V is the mean flow velocity, d the pipe diameter, and ν the kinematic viscosity ($\nu = 10^{-6}\,\mathrm{m}^2/\mathrm{s}$ in water). Figure 1 illustrates a flow generated by a fluid moving relative to a regular grid.

In general, if an obstacle of size L is placed in a fluid of kinematic viscosity ν that is moving with velocity V, a turbulent wake emerges above some critical Reynolds number $Re \equiv VL/\nu$. If the viscosity is not too high, at large Re, perturbations produced at scale L due to the nonlinear effects generate smaller and smaller scales until viscous dissipation terminates the process at a scale much smaller than L. This is the key process in turbulence: the generation of a wide range of scales in which there is neither forcing nor dissipation. This range is referred to as the *inertial interval*. The kinetic energy is transferred from the scale L, at which it is injected into the flow, to much smaller scales where viscous dissipation dominates over the nonlinearity. The process of

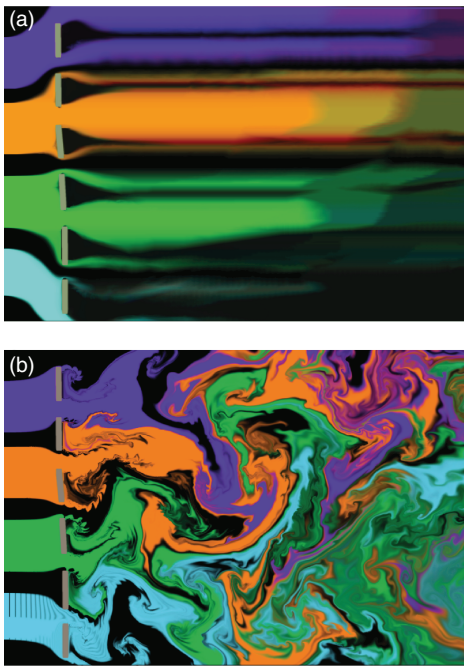

Figure 1. Fluid flowing through a grid (a) at low speed and (b) at high speed. The color-smoke pattern illustrates one of the most important roles played by turbulence, the mixing. The plots were generated using Wind Tunnel Pro application on iPad (http://windtunnelapp.com/Wind_tunnel_app/HOME.html), which simulates incompressible and homogeneous fluid motion with the Navier–Stokes equations.

the energy transfer from large to small scales is known as the direct *energy cascade*.

In the ocean, turbulence promotes the transfer of momentum and heat at the rates far greater than it would in laminar flows. It disperses particles and living organisms on the ocean surface and stirs and spreads the chemicals dissolved in the seawater. In other words, turbulence largely controls both horizontal and vertical transport in the ocean and in the atmosphere, and it is also responsible for stirring and mixing.

The eddying motions, intrinsic to turbulence, transfer momentum across fixed surfaces. The rate of such transfer is given by the time-averaged product of the transferred quantity (e.g., horizontal momentum) and the component of the turbulent velocity normal to the surface (e.g., vertical velocity fluctuations). If we denote the horizontal and vertical velocity fluctuations by $\widetilde{V}_{x,y}$ and $\widetilde{V}_z$, respectively, then the vertical flux of the horizontal momentum across a horizontal surface is given by the *Reynolds stress* of the upper fluid layer on the lower:

$$\tau = -\langle \rho \widetilde{V}_{x,y} \widetilde{V}_z \rangle \approx -\rho \langle \widetilde{V}_{x,y} \widetilde{V}_z \rangle \tag{1}$$

where ρ is the fluid density. It is clear that if the x, y, and z velocity fluctuations are not correlated, Reynolds stress is zero. The transfer of momentum can be related to the mean velocity gradient $\mathrm{d}\overline{V}/\mathrm{d}z$ through a so-called *eddy viscosity* coefficient, K, as

$$\langle \rho \widetilde{V}_{x,y} \widetilde{V}_z \rangle = K \mathrm{d}\overline{V}/\mathrm{d}z \tag{2}$$

2 INCOMPRESSIBLE 3D TURBULENCE

Incompressible fluid flow is described by the Navier–Stokes equation

$$\frac{\mathrm{d}\boldsymbol{V}}{\mathrm{d}t} = \frac{\partial \boldsymbol{V}}{\partial t} + (\boldsymbol{V} \cdot \nabla)\boldsymbol{V} = -\frac{1}{\rho}\nabla p + \nu \nabla^2 \boldsymbol{V} \tag{3}$$

(where p is the pressure) and the continuity equation,

$$\frac{\partial \rho}{\partial t} + \nabla \cdot (\rho \boldsymbol{V}) = 0 \tag{4}$$

which for the incompressible flows gives

$$\nabla \cdot \boldsymbol{V} = 0 \tag{5}$$

A system of equations 3 and 5 constitutes Navier–Stokes equations of incompressible fluid.

At large Reynolds numbers the nonlinearity is much larger than the viscous dissipation, $|(\nabla \cdot \boldsymbol{V})\boldsymbol{V}| \gg \nu \nabla^2 \boldsymbol{V}$. This is true for large scales. However, since the nonlinearity increases linearly with the wave number $k = 2\pi/l$, $|(\nabla \cdot \boldsymbol{V})\boldsymbol{V}| \sim kV^2$, while the viscous dissipation is proportional to k^2, $\nu \nabla^2 \boldsymbol{V} \sim \nu k^2$, at large k (small scales) the dissipation eventually takes over and terminates the direct energy cascade.

The idea of the energy flow from larger to smaller scales suggested by L.F. Richardson (1922) led to the concept of the *inertial interval* and of the *energy cascade* as a process, which spreads energy from large scales where it cannot be dissipated toward small scales where it can be dissipated. In the inertial interval of scales l there are no sources or sinks of energy, such that the energy flux in the wave number space stays constant. If energy is injected into a flow at a large scale L, it will then be passed on to smaller scales l until ultimately it is dissipated at some dissipation scale η whose value depends on viscosity ν. This flux of energy should naturally be equal to the energy dissipation rate ε.

Encyclopedia of Maritime and Offshore Engineering, online © 2017 John Wiley & Sons, Ltd.

DOI: 10.1002/9781118476406.emoe074
Also published in the *Encyclopedia of Maritime and Offshore Engineering* (print edition) ISBN: 978-1-118-47635-2

3 KOLMOGOROV THEORY OF TURBULENCE

In 1941, A.N. Kolmogorov in three short papers formulated (Friendlander and Topper, 1961) what is known now as *Kolmogorov theory* of turbulence, or K-41.

To summarize it, we first need to introduce velocity structure functions of the order n, which are defined as:

$$S_n(\boldsymbol{r},t) = \langle[(\boldsymbol{V}(\boldsymbol{r},t) - \boldsymbol{V}(0,t)) \cdot \boldsymbol{r}/r]^n\rangle = \langle(\delta V_L)^n\rangle \qquad (6)$$

Here, the expression in square brackets is the increment (δV_L) across the distance $\boldsymbol{r}$ in the flow of the fluctuating velocity component parallel to $\boldsymbol{r}$, and the angular brackets denote ensemble averaging over all such pairs in the flow. See also Figure 2. An nth-order velocity structure function $S_n(\boldsymbol{r},t)$ is often referred to as the nth velocity moment.

The relationship between S_2 and S_3 is known as the *Karman–Howarth relation*, and it is given by (Landau and Lifshits, 1987)

$$\frac{\partial S_2}{\partial t} = -\frac{1}{3r^4}\frac{\partial}{\partial r}(r^4 S_3) + \frac{4\varepsilon}{3} + \frac{2\nu}{r^4}\frac{\partial}{\partial r}\left(r^4\frac{\partial S_2}{\partial r}\right) \qquad (7)$$

Here again, $\varepsilon = \nu(\nabla \boldsymbol{V})^2$ is the mean energy dissipation rate. From this relation, in steady state $(\partial S_2/\partial t = 0)$, one can derive for the third-order structure function: $S_3(r) = -4\varepsilon r/5 + 6\nu(\mathrm{d}S_2(r)/\mathrm{d}r)$. Kolmogorov considered a limit of vanishing viscosity ν and assumed that ε is nonzero to obtain the so-called 4/5 law:

$$S_3(r) = -\frac{4}{5}\varepsilon r \qquad (8)$$

The 4/5 law is obtained as a direct consequence of the Navier–Stokes equations. This law relates the third-order structure function of velocity fluctuations and the energy flux through inertial interval. If the range of scales r is larger than the Kolmogorov dissipation scale $\eta = \nu^{3/4}\varepsilon^{1/4}$ and smaller than the energy injection scale L, the flux is constant for all r and does not depend on viscosity.

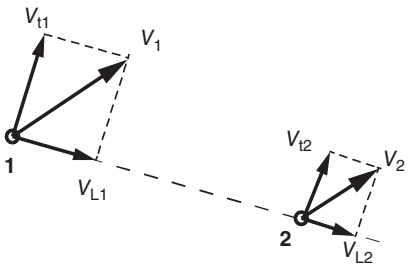

Figure 2. Computation of the velocity increments for structure functions estimations.

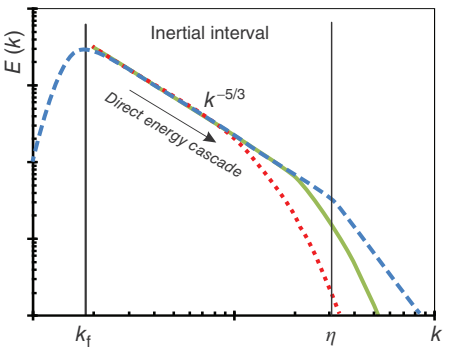

Figure 3. Kinetic energy spectrum of three-dimensional turbulence. Dotted line corresponds to the highest viscosity, while dashed line corresponds to lower viscosity.

For the second-order structure function dimensional analysis gives:

$$S_2(r) \propto C_2\langle\varepsilon\rangle^{2/3} r^{2/3} \qquad (9)$$

This expression (sometimes also called a *2/3 law*) can be rewritten in Fourier space to give a famous Kolmogorov spectrum of kinetic energy (Figure 3):

$$E(k) = C_K\langle\varepsilon\rangle^{2/3} k^{-5/3} \qquad (10)$$

where k is the wave number corresponding to a scale l, and C_k is the Kolmogorov constant. In 3D turbulence, $C_K \approx 0.5$ (Sreenivasan, 1995).

4 KOLMOGOROV PHENOMENOLOGY OF TURBULENCE

The results of the K-41 theory formed a framework in which relations between turbulence parameters can be established on the basis of exact results (such as 4/5 law), empirical laws (e.g., 2/3 law), and dimensional considerations. Such phenomenological approach seems very useful in many applications where qualitative relation between flow statistical variables need to be established.

The main parameters in the turbulence phenomenology are: the scale l, the velocity associated with this scale, V_l, the r.m.s. velocity fluctuation, V_L, and the eddy turnover time associated with the scale l, $\tau_l = l/V_L$. The eddy turnover time reflects the time of transfer of excitation in incompressible fluid. It can be used to estimate the energy flux from scale l to smaller scales. It is defined as the amount of kinetic energy per mass, V_l^2, associated with the eddy of scale l, transferred to smaller scales in the typical time τ_l: $\Pi_l = V_l^2/\tau_l = V_l^3/l$.

Encyclopedia of Maritime and Offshore Engineering, online © 2017 John Wiley & Sons, Ltd.

DOI: 10.1002/9781118476406.emoe074
Also published in the *Encyclopedia of Maritime and Offshore Engineering* (print edition) ISBN: 978-1-118-47635-2

This flux in the inertial interval (no energy injection, nor dissipation) equals to the energy dissipation rate ε: $\Pi_l = \varepsilon$. From this, it follows that the velocity of the scale l is the scale invariant of exponent $h = 1/3$:

$$V_l = \varepsilon^{1/3} l^{1/3} \tag{11}$$

This gives another expression for the eddy turnover time:

$$\tau_l = \varepsilon^{-1/3} l^{2/3} \tag{12}$$

The latter expression can be used in practical applications to distinguish between coherent vortices (with long life time), often present in turbulent flows and turbulence eddies constituting Kolmogorov spectrum of kinetic energy.

Near the top of the inertial interval, where $l \sim L$, Equation 11 gives $V_L = \varepsilon^{1/3} L^{1/3}$, and

$$\varepsilon = V_L^3 / L \tag{13}$$

At the end of the inertial interval, where viscosity becomes important, the characteristic scales can be obtained as follows (Frisch, 1995). The typical time to attenuate excitation at the scale l by viscous diffusion is $\tau_l^d = l^2/\nu$. This diffusive time decreases faster with the decrease in l than the eddy turnover time (Equation 12). It means that at any small viscosity there will be sufficiently small scale η, at which τ_l^d will become shorter than τ_l:

$$\eta = \left(\frac{\nu^3}{\varepsilon} \right)^{1/4} \tag{14}$$

which is the Kolmogorov dissipation scale discussed above.

Using Equations 13 and 14, one can arrive at a very important relationship between the forcing scale L, Kolmogorov dissipation scale η, and the Reynolds number, $R = (V_L L)/\nu$:

$$\frac{L}{\eta} \sim \left(\frac{\nu^3}{V_L^3 L^3} \right)^{-1/4} \sim R^{3/4} \tag{15}$$

The ratio L/η, which characterizes the extent of the inertial interval, grows as $R^{3/4}$. This allows estimating the size of the computational grid in numerical simulations of turbulence. In three-dimensional (3D) model, the minimal number of grid points should be $N \sim (L/\eta)^3$. The relation 15 suggests that the size of the computational grid grows as $N \sim R^{9/4}$. This highlights the difficulty of achieving high Reynolds numbers in direct numerical simulations (DNS) of turbulence. Sometimes this estimate ($R^{9/4}$) is used as a measure of the number of degrees of freedom of turbulence.

5 NUMERICAL SIMULATION OF TURBULENCE

Though the Navier–Stokes equations 3 and 5 are the deterministic ones and allow, in principle, computing any turbulent flow given the initial and boundary conditions, a very large number of degrees of freedom (see above) makes this task impossible in many practical situations. As mentioned before, turbulence is characterized by a broad range of scales. In 3D turbulence, the kinetic energy is contained in scales that are much larger than the energy-dissipating scales.

DNS. In this computational method all scales are taken into account, including the smallest scales where the kinetic energy is dissipated. Since the ratio of the integral scale and the dissipation scale is proportional to $R^{3/4}$, the number of grid points needed to simulate a cube whose size equals to the integral scale is $N_g \sim R^{9/4}$. For values of $R = 10^8$, typical, for example, for turbulent clouds, one would need a computational grid of 10^{18} points! In the boundary layer of a large aircraft $R \sim 6 \times 10^5$, which gives $N \sim 10^{13}$. These examples illustrate that most of practically important problems in turbulence cannot be addressed in DNS, at least in the near future. This highlights the role of alternative approaches to numerical simulations of turbulence as well as the importance of laboratory experiments and new theoretical approaches in turbulence studies.

Large-eddy simulations (LES). To reduce the grid size needed for DNS, another method of turbulence simulation, LES, is often used in which the equations of motion are space averaged. To implement this space averaging, the variables are filtered,

$$\overline{V}_i = \int Q(\mathbf{x} - \mathbf{x}') V_i(\mathbf{x}') \mathrm{d}\mathbf{x}' \tag{16}$$

where $Q(\mathbf{x})$ is the smoothing kernel. This kernel can be, for example, the box filter,

$$Q(\mathbf{x}) = \begin{array}{l} 1/\sigma, \text{ if } |\mathbf{x}| < \sigma/2 \\ 0\,, \quad \text{if } |\mathbf{x}| > \sigma/2 \end{array}$$

or the Gaussian filter

$$Q(\mathbf{x}) = \frac{1}{\sigma\sqrt{2\pi}} \mathrm{e}^{-x^2/2\sigma^2}$$

The main idea of the method is to avoid computing the dissipation scales and also the scales in the inertial interval, which are assumed isotropic and equilibrium. This is possible if the energy transfer is known. The large scales are computed directly, while other scales are substituted by a subgrid model. Space-averaged variables are local averages, somewhat similar to the representation of the turbulent velocity as a sum of the mean and the fluctuation:

Encyclopedia of Maritime and Offshore Engineering, online © 2017 John Wiley & Sons, Ltd.

DOI: 10.1002/9781118476406.emoe074
Also published in the *Encyclopedia of Maritime and Offshore Engineering* (print edition) ISBN: 978-1-118-47635-2

$V_i(\mathbf{x}, t) = \overline{V}_i(\mathbf{x}) + \widetilde{V}_i(\mathbf{x}, t)$. In Fourier space, smoothing filters damp higher wave numbers, while lower ones remain almost unaffected. Effectively, filtering separates large eddies, containing the energy from the Reynolds stresses, and subgrid components containing the dissipation.

Applying filtering of variables to the incompressible Navier–Stokes equations gives

$$\frac{\partial \overline{V}_i}{\partial t} + \frac{\partial(\overline{V}_i \overline{V}_j)}{\partial x_j} = -\frac{1}{\rho}\frac{\partial p^*}{\partial x_i} + \frac{\partial}{\partial x_j}\left(\nu \frac{\partial \overline{V}_i}{\partial x_j} + \overline{\tau}_{ij}\right)$$

$$\frac{\partial \overline{V}_i}{\partial x_j} = 0 \tag{17}$$

where the Reynolds stress $\overline{\tau}_{ij} = T_{ij} - (T_{kk}/3)\delta_{ij}$, $T_{ij} = \overline{V}_i \overline{V}_j - V_i V_j$, and $p^* = \overline{p} - \rho T_{kk}/3$ is a modified pressure. The subgrid stresses can be assumed to be proportional to the filtered rate-of-strain tensor

$$\overline{\tau}_{ij} = 2\nu_\varepsilon \overline{S}_{ij} \tag{18}$$

where ν_ε is the subgrid eddy viscosity and $\overline{S}_{ij}$ the rate-of-strain tensor computed with the filtered velocity.

Reynolds-averaged Navier–Stokes simulations (RANS). This method for computing turbulent flows requires solving directly the Reynolds-averaged Navier–Stokes equations:

$$\frac{\partial \overline{V}_i}{\partial t} + \frac{\partial(\overline{V}_i \overline{V}_j)}{\partial x_j} = -\frac{1}{\rho}\frac{\partial p}{\partial x_i} + \frac{\partial}{\partial x_j}\left(\nu \frac{\partial \overline{V}_i}{\partial x_j} - \langle \widetilde{V}_i \widetilde{V}_j \rangle\right)$$

$$\frac{\partial \overline{V}_i}{\partial x_j} = 0 \tag{19}$$

The main difficulty intrinsic to this method is the presence of unknown Reynolds stresses $\langle \widetilde{V}_i \widetilde{V}_j \rangle$, which requires finding an appropriate closure.

6 TWO-DIMENSIONAL TURBULENCE

If the fluid depth is small, large-scale motions can be approximated as two dimensional (2D). For example, intermediate range motions in the atmosphere and in the ocean are larger than their corresponding depths. In this section, we will discuss how realistic such an assumption can be in laboratory and natural flows. We will show that, surprisingly, properties of 2D turbulence are found in a variety of turbulent flows, which cannot *a priori* be thought as 2D. The Navier–Stokes equations for an incompressible 2D flow, whose velocity field is $\mathbf{V}(\mathbf{r}, t) = [V_x(x, y, t), V_y(x, y, t)]$, are given as

$$\frac{\partial \mathbf{V}}{\partial t} + \mathbf{V} \cdot \nabla \mathbf{V} = -\frac{1}{\boldsymbol{\rho}} \nabla p + \nu \nabla^2 \mathbf{V} - \alpha \mathbf{V} + f_{\mathbf{V}} \tag{20}$$

where $f_{\mathbf{V}}$ is a forcing and α characterizes linear frictional damping. This can be rewritten for the vorticity $\omega = \nabla \times \mathbf{V} = -\nabla^2 \psi$, which in a 2D flow is a scalar, as

$$\frac{\mathrm{d}\omega}{\mathrm{d}t} = \nu \nabla^2 \omega - \alpha \omega + f \tag{21}$$

where $\mathrm{d}\omega/\mathrm{d}t = \partial\omega/\partial t + \mathbf{V} \cdot \nabla\omega$ and $f = \nabla \times f_{\mathbf{V}}$. If viscosity is zero, $\nu = 0$, vorticity is conserved in the absence of forcing and dissipation, $\mathrm{d}\omega/\mathrm{d}t = 0$. In this case, the flow has two conserved quantities, or two quadratic invariants, the kinetic energy $E = (1/2)\langle V^2 \rangle$ and *enstrophy*, or squared vorticity, $\Omega = (1/2)\langle \omega^2 \rangle$. The existence of these two invariants, as was suggested by Kraichnan (1967), leads to the existence of two turbulent cascades in 2D: the *inverse energy cascade* and the *direct enstrophy cascade*. In other words, in contrast to the direct energy cascade in three dimensions, 2D turbulence supports spectral energy transfer from smaller to larger scales. Kolmogorov's assumption that the energy spectrum $E(k)$ depends only on the wave number k and on the energy dissipation rate ε leads to the same spectrum in the energy cascade range as in 3D turbulence, Figure 4:

$$E(k) = C\varepsilon^{2/3} k^{-5/3},\ k < k_{\mathrm{f}} \tag{22}$$

where $E(k)$ is defined such that the mean kinetic energy per unit mass is given by

$$E = \int_0^\infty E(k)\mathrm{d}k \tag{23}$$

and $C \approx 6$ is a constant. A similar assumption that the squared vorticity spectrum depends only on the enstrophy dissipation rates ε_ω and k leads to the spectrum shape in the direct enstrophy cascade range given by

$$E(k) = C' {\varepsilon_\omega}^{2/3} k^{-3},\ k > k_{\mathrm{f}} \tag{24}$$

The exact relation for the third-order structure function holds in 2D turbulence, giving an equivalent of Equation 8 of the 3D Kolmogorov 4/5 law (Yakhot, 1999):

$$S_{3L}(r) = \langle [\delta V_L]^3 \rangle = \frac{3}{2}\varepsilon r \tag{25}$$

Note that in 2D turbulence, the third-order structure function is positive, indicating the direction of the energy flux opposite to that in 3D, that is, from smaller to larger scales.

6.1 Spectral condensation in 2D turbulence

The existence of the inverse energy cascade in 2D turbulence gives it an amazing ability to self-organize. This can

Encyclopedia of Maritime and Offshore Engineering, online © 2017 John Wiley & Sons, Ltd.

DOI: 10.1002/9781118476406.emoe074
Also published in the *Encyclopedia of Maritime and Offshore Engineering* (print edition) ISBN: 978-1-118-47635-2

be observed as the transition from highly irregular chaotic motion dominated by eddies of different scales to the flow dominated by one or several vortices coherent across the bounded domain. This phenomenon, referred to as *spectral condensation of energy*, was predicted by Kraichnan (1967), who likened this phenomenon to a Bose–Einstein condensation in quantum gases.

In the presence of the large-scale or uniform dissipation (e.g., bottom drag), energy delivered to large scales will be dissipated. The maximum of the spectrum in this case will stabilize at some dissipation wave number given by $k_\alpha \approx 2\pi(\alpha^3/\varepsilon)^{1/2}$, see Figure 4. If however the flow is bounded, such that the box size is $L < 2\pi/k_\alpha$, energy will start to accumulate at the scale comparable to L until the energy input through the inverse energy cascade is balanced by the dissipation. A large coherent vortex will develop and will exist in steady state, as illustrated in Figure 5. The kinetic energy spectrum in the presence of a condensate becomes steep, $E(k) \sim k^{-3}$; however, when the coherent vortex is subtracted out, the spectrum reveals underlying turbulence with $E(k) \sim k^{-5/3}$ (Xia, Shats, and Falkovich, 2009).

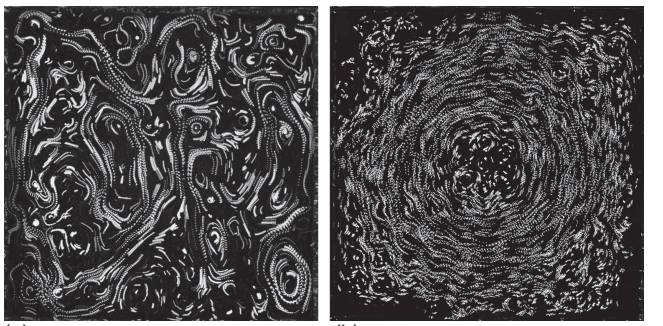

Figure 5. Spectral condensation of 2D turbulence in laboratory experiments (Xia, Shats, and Falkovich, 2009) is observed as the aggregation of turbulent eddies of different scales (a) into a coherent vortex (b), which dominates the flow and is sustained by the inverse energy cascade.

6.2 2D turbulence in 3D flows

From the point of view of the applicability of the 2D turbulence theory to real flows in laboratory and in nature, the question is: can any real flows be 2D? The formal answer to this question is "*no*" since physical fluid systems are intrinsically 3D. However, if we recall that the main difference between 2D and 3D turbulence is the direction of the energy transfer in the inertial range, the question may be asked differently: "Can laboratory and natural turbulent flows support the inverse energy cascade?"

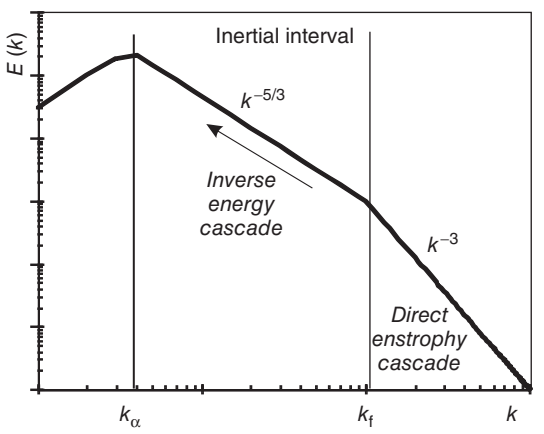

Figure 4. Kinetic energy spectrum of two-dimensional turbulence. k_f is the forcing scale wave number, while k_α characterizes large-scale dissipation.

Recent studies in a surprisingly broad range of turbulent flows answer this question positively. Early laboratory experiments aiming to test main predictions of the 2D turbulence theory were performed by forcing turbulence electromagnetically in thin layers of electrolytes (Sommeria, 1986; Paret and Tabeling, 1997) and using falling soap films (Couder, Chomaz, and Rabaud, 1989; Gharib and Derango, 1989). The main idea was to constrain motion in one spatial dimension (depth). Later, it was found that in thick fluid layers (depth larger that the turbulence forcing scale) the planarity of flows could be imposed on smaller scales by large-scale coherent flows (Xia *et al*., 2011). Such large-scale flows can either be self-generated by turbulence in the process of spectral condensation, or they can be externally imposed on turbulence.

Such a scenario has been later confirmed in the energy dynamics of the hurricane boundary layer (Byrne and Zhang, 2013). The hurricane, representing a large-scale coherent vortex, imposes two dimensionality onto boundary layer turbulence turning it from 3D into 2D. The direction of the energy transfer changes with the height from the direct cascade (from large to small scales) in 3D to the inverse energy cascade (from small to large scales) in 2D. As a result, the large vortex may gain energy from small scales.

A possibility of the inverse energy cascade in 3D isotropic turbulence has been studied in numerical simulations of the Navier–Stokes equations (Biferale, Musacchio, and Toschi, 2012) where it has been shown that the inverse turbulent spectral transfer may be due to the interactions between velocity components carrying a well-defined helicity. The inverse energy cascade thus is not necessarily connected to a two-dimensionalization of the flow.

Encyclopedia of Maritime and Offshore Engineering, online © 2017 John Wiley & Sons, Ltd.

DOI: 10.1002/9781118476406.emoe074
Also published in the *Encyclopedia of Maritime and Offshore Engineering* (print edition) ISBN: 978-1-118-47635-2

Another example of the 2D turbulence was recently found in the motion of the floaters on the surface of liquids perturbed by the Faraday waves (von Kameke *et al*., 2011; Francois *et al*., 2013). Though the floaters motion is 3D, the statistics of their horizontal motion is identical to those of the 2D turbulence, including the observation of the inverse energy cascade and of the direct enstrophy cascade in the kinetic energy spectra, Equations 23 and 24, the observation of the linear positive third-order structure functions of the velocity increments, Equation 25, and spectral condensation of energy.

7 LAGRANGIAN STATISTICS OF TURBULENCE

7.1 Lagrangian versus Eulerian description

The Lagrangian description of fluid flows, in which the observer follows the fluid particles wherever they move, is physically more natural than the Eulerian one in which the observers are at fixed spatial positions, since it is related to the motion of fluid elements, or matter. Though in the past technical difficulties hindered the use of the Lagrangian approach in turbulent flows, recent progress in computational power and in the laboratory imaging tools led to a focused effort in studying turbulence from Lagrangian perspective.

In the Eulerian frame, the flow characteristics are functions of coordinates $\mathbf{X}$ and time t. The flow velocity is given by a function $\mathbf{u}_{\mathrm{E}}(\mathbf{X}, t)$ measured at a position $\mathbf{X}$ at time t.

In the Lagrangian description, fluid particles' positions are followed in time. If we define a position of a particle at some initial time t_0 as $\mathbf{X}_0$, the flow is described by a function $\mathbf{X}(\mathbf{X}_0, t)$, giving the position of the particle at time t.

The two descriptions are related as follows:

$$\frac{\partial \mathbf{X}(t|\mathbf{X}_0, t_0)}{\partial t} = \mathbf{u}_{\mathrm{L}}(t|\mathbf{X}_0, t_0)$$
$$\mathbf{u}_{\mathrm{L}}(t|\mathbf{X}_0, t_0) = \mathbf{u}_{\mathrm{E}}((\mathbf{X}(t)|\mathbf{X}_0, t_0), t) \qquad (26)$$

where indices "L" and "E" refer to the Lagrangian and Eulerian quantities, respectively.

The relation between Eulerian and Lagrangian fields is a difficult (if solvable) mathematical problem. The main difficulty is that the Lagrangian field $\mathbf{X}(\mathbf{X}_0, t)$ is a complicated functional of the Eulerian velocity field $\mathbf{u}_{\mathrm{E}}(\mathbf{X}, t)$. If the Eulerian velocity field is known or given, Equation 26 serves for determination of a trajectory of a fluid particle with the initial position $\mathbf{X}_0$. This equation is nonlinear even for very simple fluid flows and is generically nonintegrable. Even if the Eulerian velocity $\mathbf{u}_{\mathrm{E}}(\mathbf{X}, t)$ is regular and laminar, the Lagrangian velocity $\mathbf{u}_{\mathrm{E}}(\mathbf{X}(t|\mathbf{X}_0, t_0), t)$ can be chaotic because the trajectory is chaotic. Thus, a flow can be laminar in the Eulerian sense, but chaotic or turbulent in the Lagrangian sense (Tsinober, 2001).

Lagrangian measurements can be obtained from numerical simulations, laboratory experiments, and from measurements in the atmosphere and in the ocean.

In numerical simulations, a well-resolved instantaneous velocity field evolving according to the Navier–Stokes equations must be available. The interpolation scheme needs to be reasonably efficient when large numbers of particles are tracked. Finally, a sufficient number of particles with high degree of statistical independence should be tracked and included in the ensemble averages.

In experiments, the essential task is to obtain records of the particle positions over time using optical or other particle-detection techniques. Then Equation 26 can be used in reverse to obtain the particle velocity. The main difficulty here is to locate a particle while maintaining its identity for a significant period of time. Recent advances in experimental tools and techniques allow obtaining high-quality Lagrangian data in laboratory (Toschi and Bodenschatz, 2009). Alternatively, particle trajectories can be simulated from the measured velocity fields in the flow.

7.2 Particle motion in turbulent fluids

Classical descriptions of Lagrangian dynamics involve statistical analysis of trajectories of individual particles ($N = 1$) following the work of Taylor (1921) and of the relative displacement of two trajectories ($N = 2$) following the work of Richardson (1926). Later, studies of the particle dispersion in turbulence extended toward multiparticle dynamics, which are of interest from the point of view of the evolution of fluid patches (groups of N fluid elements with $N > 2$) (Falkovich, Gawedzki, and Vergassola, 2001; Xu, Ouellette, and Bodenschatz, 2008).

7.3 Single-particle dispersion

The most basic property of Lagrangian trajectories is a single-particle dispersion, or mean squared displacement $\langle \delta r^2 \rangle = \langle |\mathbf{r}(t) - \mathbf{r}(t_0)|^2 \rangle$ of a particle moving along the trajectory $\mathbf{r}(t)$ from its initial position $\mathbf{r}(t_0)$ over time interval $\delta t = (t - t_0)$, Figure 6. It can be shown that

$$\frac{\partial}{\partial t}\langle \delta r^2 \rangle = 2\boldsymbol{u}(t) \cdot \int_{t_0}^{t} \boldsymbol{u}(s)\mathrm{d}s \qquad (27)$$

Encyclopedia of Maritime and Offshore Engineering, online © 2017 John Wiley & Sons, Ltd.

DOI: 10.1002/9781118476406.emoe074
Also published in the *Encyclopedia of Maritime and Offshore Engineering* (print edition) ISBN: 978-1-118-47635-2

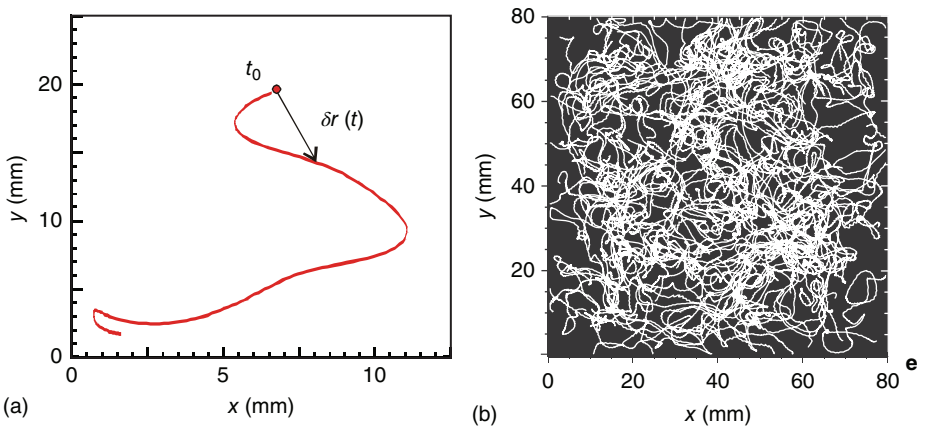

Figure 6. Particle trajectories in turbulence: (a) particle displacement from its initial position in the flow and (b) tracked particle trajectories in the wave-driven 2D turbulence.

By performing the ensemble averaging and assuming velocities $\boldsymbol{u}$ statistically stationary, one can obtain an equation for the second moment of the single-particle displacement:

$$\frac{\partial}{\partial t}\langle \delta r^2 \rangle = 2\int_{t_0}^{t} \langle \boldsymbol{u}(0)\cdot\boldsymbol{u}(s)\rangle \mathrm{d}s \tag{28}$$

The behavior of $\langle(\delta r)^2\rangle$ depends on the range of temporal correlation $\langle \boldsymbol{u}(0)\cdot\boldsymbol{u}(t)\rangle$ of the Lagrangian velocity $\boldsymbol{u}(t)$. The Lagrangian velocity correlation time is defined as

$$T_{\mathrm{L}} = \frac{1}{\langle \boldsymbol{u}^2\rangle}\int_{t_0}^{\infty} \langle \boldsymbol{u}(0)\cdot\boldsymbol{u}(t)\rangle \mathrm{d}t = \int_{t_0}^{\infty} \mathrm{d}t \frac{\rho(t)}{\langle \boldsymbol{u}^2\rangle} \tag{29}$$

Here, $\rho(t)$ is the Lagrangian velocity autocorrelation function. The value of T_{L} provides a measure of the Lagrangian velocity memory. For times $t \ll T_{\mathrm{L}}$, the two-time correlation function in Equation 28 approximately equals $\langle u^2\rangle$ and the particle transport is ballistic (displacement linearly proportional to time). At longer times, $t \gg T_{\mathrm{L}}$, when the Lagrangian correlation time is finite, diffusive regime arises, such that the mean displacement scales a square root of time (Taylor, 1921):

$$\begin{aligned} \langle(\delta r)^2\rangle &= \langle u^2\rangle t^2 \quad t \ll T_{\mathrm{L}} \\ \langle(\delta r)^2\rangle &= 2\langle u^2\rangle T_{\mathrm{L}} t \quad t \gg T_{\mathrm{L}} \end{aligned} \tag{30}$$

The particle displacements over time segments spaced by distances much larger than T_{L} are almost independent. At long times, the displacement δr behaves as a sum of many independent variables and falls into a class of stationary processes governed by the Central Limit Theorem. In other words, the displacement for $t \gg T_{\mathrm{L}}$ becomes similar to a Brownian motion. Taylor's single-particle dispersion,

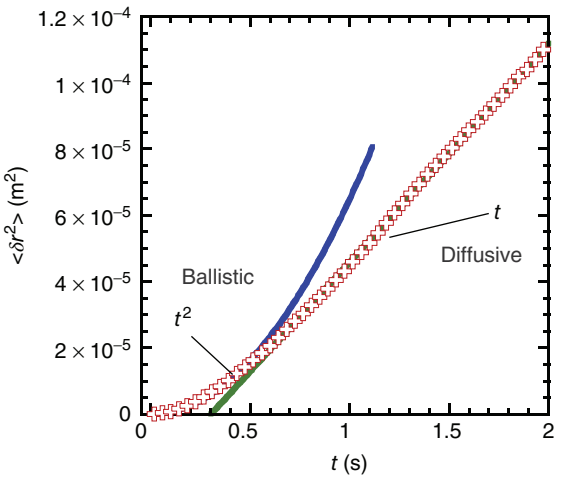

Figure 7. Experimental confirmation of the Taylor's single-particle dispersion, Equation 30, in two-dimensional turbulence. (Reproduced with permission from Xia *et al.*, 2013. © Nature publishing, 2013.)

Equation 30, has been confirmed in laboratory experiments in 2D turbulence in both ballistic and diffusive regimes (Xia *et al.*, 2013; Figure 7).

The timescale T_{L} corresponds to a distance $L_{\mathrm{L}} = \langle u\rangle T_{\mathrm{L}}$, the Lagrangian eddy length scale. By analogy with Fickian diffusion, $\langle(\delta r)^2\rangle$ can be related to an effective eddy diffusivity $\kappa_{\mathrm{H}} = \frac{1}{2}\frac{\mathrm{d}}{\mathrm{d}t}\langle(\delta r)^2\rangle$, which asymptotes to $\kappa_{\mathrm{H}} = \langle u\rangle L_{\mathrm{L}}$ or $\kappa_{\mathrm{H}} = \langle u^2\rangle T_{\mathrm{L}}$ in the random walk limit $t \gg T_{\mathrm{L}}$.

To estimate the diffusion coefficient κ_{H}, one needs to compute or to measure the Lagrangian velocity autocorrelation function $\rho(t)$. However, $\rho(t)$ and T_{L} cannot be theoretically predicted. In some cases it is possible to rely on the empirically found relationships, such as the one recently reported for laboratory 2D turbulence (Xia *et al.*, 2013). If 2D turbulence is fully developed, and the velocity

Encyclopedia of Maritime and Offshore Engineering, online © 2017 John Wiley & Sons, Ltd.

DOI: 10.1002/9781118476406.emoe074
Also published in the *Encyclopedia of Maritime and Offshore Engineering* (print edition) ISBN: 978-1-118-47635-2

autocorrelation function is a decaying exponential in time, $\rho(t) \sim \exp\{-t/T_L\}$, the mean-squared displacement in 2D turbulence is determined by the turbulence forcing scale L_f as

$$\langle \delta r^2 \rangle = \frac{L_f^2}{T_L} t, \quad t \gg T_L \tag{31}$$

7.4 Particle pair dispersion

Along with single-particle dispersion, the dynamics of a pair of initially adjacent particles in a flow is of interest in such problems as spreading of pollutants. Relative dispersion in turbulence was considered by Richardson (1926), who, based on the experimental data in the atmosphere, obtained a celebrated Richardson law (1926) for the separation distance $R(t)$ between two particles with time as

$$\langle [R(t)]^2 \rangle \sim t^3 \tag{32}$$

By applying Kolmogorov's scaling theory, Obukhov (1941) postulated that in the inertial range of turbulence, the pair dispersion should grow as $\langle [R(t)]^2 \rangle \sim g\varepsilon t^3$ g, where g is a universal constant. Batchelor (1952) refined this work, predicting that the mean-square separation should grow as $\langle [R(t)]^2 \rangle \sim \frac{3}{11} C_2 (\varepsilon r_0)^{2/3} t^2$ for times shorter than a characteristic timescale t_0, which depends on the initial separation of the pair r_0.

The pair dispersion between two fluid particles with trajectories $R_n(t) = R(t, r_n)$ can simplistically be described by the evolution equation for the interparticle distance $\mathbf{R}_{12} = \mathbf{r}_1 - \mathbf{r}_2$ as:

$$\frac{d\mathbf{R}_{12}}{dt} = \Delta V_{||} \tag{33}$$

where $\Delta V_{||} = \mathbf{u}_{1||} - \mathbf{u}_{2||}$ is the longitudinal velocity difference (computed along $\mathbf{R}_{12}$). In developed turbulence, $\Delta V_{||}$ can be estimated from the Kolmogorov 4/5 law: $\langle \Delta V_{||} \rangle^3 = -\frac{4}{5}\varepsilon r$. Then, $\Delta V_{||} \propto R^{1/3}$ and $\frac{d\langle \mathbf{R}_{12} \rangle}{dt} \propto R^{1/3}$, or in a more general case

$$\frac{d\langle \mathbf{R}_{12} \rangle}{dt} \propto R^{\alpha} \quad \alpha < 1 \tag{34}$$

For $\alpha = 1/3$, $\langle R^2 \rangle \sim t^3$, which is the Richardson's Law (1926).

8 CONCLUSIONS

We discussed fundamental concepts, which are used to describe turbulent flows. Particular attention is paid to the Kolmogorov theory of homogeneous isotropic 3D turbulence in incompressible fluid, which is based on the Richardson's idea of energy cascade. A brief review of numerical modeling of turbulence is given. Recent progress in understanding the robustness of 2D turbulence makes it by far more ubiquitous than it was initially thought. In particular, the identification of 2D turbulence in 3D flows, such as thick fluid layers, or on the surface of water perturbed by waves, opens numerous opportunities to apply understanding of 2D turbulence to geophysical flows. The role of turbulence in mixing and dispersion of matter is best characterized using Lagrangian statistics. Overall, we just scratched the surface in this fast-developing field of modern science.

GLOSSARY

Energy cascade	A multi-step energy transfer process between scales in turbulent flows.
Enstrophy	Integral of the square of the vorticity.
Inertial interval	A range of scales or wave numbers in which energy is transferred from scale to scale without forcing or dissipation.
Inverse cascade	Spectral energy transfer from smaller to larger scales in two-dimensional turbulence.
Kolmogorov scale	A dissipative scale at which turbulent cascade in three-dimensional turbulence is terminated.
Pair dispersion	A statistical law of separation of two initially close fluid particles in a flow.
Single particle dispersion	A law determining how fast a fluid particle in a flow moves away from its initial position.
Spectral condensation	The accumulation of turbulent energy at the scales close to the boundary box size in two-dimensional turbulence.

RELATED ARTICLES

Characteristics of Viscous, Rotational and Irrotational Flows
Wave Boundary Layer in the Lower Atmosphere

REFERENCES

Batchelor, G.K. (1952) Diffusion in a field of homogeneous turbulence. *Proceedings of the Cambridge Philosophical Society*, **48**, 345–362.

Biferale, L., Musacchio, S., and Toschi, F. (2012) Inverse energy cascade in three-dimensional isotropic turbulence. *Physical Reviews Letters*, **108**, 164501.

Encyclopedia of Maritime and Offshore Engineering, online © 2017 John Wiley & Sons, Ltd.

DOI: 10.1002/9781118476406.emoe074
Also published in the *Encyclopedia of Maritime and Offshore Engineering* (print edition) ISBN: 978-1-118-47635-2

Byrne, D. and Zhang, J.A. (2013) Height dependent transition from three- to two-dimensional turbulence in the hurricane boundary layer. *Geophysical Research Letters*, **40**, 1439–1442.

Couder, Y., Chomaz, J., and Rabaud, M. (1989) On the hydrodynamics of soap films. *Physica D*, **37**, 384–405.

Falkovich, G., Gawedzki, K., and Vergassola, M. (2001) Particles and fields in fluid turbulence. *Reviews of Modern Physics*, **73**, 913–975.

Francois, N., Xia, H., Punzmann, H., and Shats, M. (2013) Inverse energy cascade and emergence of large coherent vortices in turbulence driven by Faraday waves. *Physical Reviews Letters*, **110**, 194501.

A.N. Kolmogorov Dokl. Akad. Nauk SSSR **30**, 301 (1941); **31**, 538 (1941); **32**, 16 (1941); in Friendlander, S.K. and Topper, L. (eds) (1961) *Turbulence, Classical Papers on Statistical Theory*, Interscience Publishers, London.

Frisch, U. (1995) *Turbulence: The Legacy of A.N. Kolmogorov*, Cambridge University Press, Cambridge, England.

Gharib, M. and Derango, P. (1989) A liquid film (soap film) tunnel to study two-dimensional laminar and turbulent shear flows. *Physica D*, **37**, 406–416.

von Kameke, A., Huhn, F., Fernández-García, G., Muñuzuri, A.P., and Pérez-Muñuzuri, V. (2011) Double cascade turbulence and Richardson dispersion in a horizontal fluid flow induced by Faraday waves. *Physical Reviews Letters*, **107**, 074502.

Kraichnan, R.H. (1967) Inertial ranges in two-dimensional turbulence. *Physics of Fluids*, **10**, 1417–1423.

Landau, L. and Lifshits, E. (1987) *Fluid Mechanics*, Pergamon Press, Oxford.

Obukhov, A.M. (1941) On the energy distribution in the spectrum of a turbulent flow. *Izvestiya Akademii Nauk SSR*, **5**, 453–466. (in Russian)

Paret, J. and Tabeling, P. (1997) Experimental observation of the two-dimensional inverse energy cascade. *Physical Reviews Letters*, **79**, 4162–4165.

Reynolds, O. (1883) An experimental investigation of the circumstances which determine whether the motion of water in parallel channels shall be direct or sinuous and of the law of resistance in parallel channels. *Philosophical Transactions of the Royal Society*, **174**, 935–982.

Richardson, L. (1926) Atmospheric diffusion shown on a distance-neighbour graph. *Proceedings of the Royal Society of London, Series A*, **110**, 709–737.

Richardson, L.F. (1922) *Weather prediction by numerical process*, Cambridge University Press.

Scott, A. (ed) (2005) *Encyclopedia of Nonlinear Science*, Taylor & Francis Group, New York, pp. 1–947.

Sommeria, J. (1986) Experimental study of the two-dimensional inverse energy cascade in a square box. *Journal of Fluid Mechanics*, **170**, 139–168.

Sreenivasan, K.R. (1995) On the universality of the Kolmogorov constant. *Physics of Fluids*, **7**, 2778–2784.

Taylor, G.I. (1921) Diffusion by continuous movements. *Proceedings of the London Mathematical Society*, **20**, 196–211.

Toschi, F. and Bodenschatz, E. (2009) Lagrangian properties of particles in turbulence. *Annual Review of Fluid Mechanics*, **41**, 375–404.

Tsinober, A. (2001) *An Informal Introduction to Turbulence*, Kluwer Academic Publishers, Dordrecht.

Xia, H., Shats, M., and Falkovich, G. (2009) Spectrally condensed turbulence in thin layers. *Physics of Fluids*, **21**, 125101.

Xia, H., Byrne, D., Falkovich, G., and Shats, M. (2011) Upscale energy transfer in thick turbulent fluid layers. *Nature Physics*, **7**, 321.

Xia, H., Francois, N., Punzmann, H., and Shats, M. (2013) Lagrangian scale of particle dispersion in turbulence. *Nature Communications*, **4**, 2013.

Xu, H., Ouellette, N., and Bodenschatz, E. (2008) Evolution of geometric structures in intense turbulence. *New Journal of Physics*, **10**, 013012.

Yakhot, V. (1999) Two-dimensional turbulence in the inverse cascade range. *Physical Review E*, **60**, 5544–5551.

FURTHER READING

Boffetta, G. and Ecke, R.E. (2012) Two-dimensional turbulence. *Annual Review of Fluid Mechanics*, **44**, 427–451.

Frisch, U. (1995) *Turbulence: The Legacy of A. N. Kolmogorov*, Cambridge University Press, Cambridge, England.

Monin, A.S. and Yaglom, A.M. (1975) *Statistical Fluid Mechanics*, Vols. 1, 2, MIT, Cambridge.

Encyclopedia of Maritime and Offshore Engineering, online © 2017 John Wiley & Sons, Ltd.

DOI: 10.1002/9781118476406.emoe074
Also published in the *Encyclopedia of Maritime and Offshore Engineering* (print edition) ISBN: 978-1-118-47635-2